Application of Landsat-7 ETM+ and MODIS products in mapping seasonal accumulation of growing degree days at an enhanced resolution

Quazi K. Hassan[1], Charles P.-A. Bourque[1, 2], and Fan-Rui Meng[1]
[1] Faculty of Forestry & Environmental Management, University of New Brunswick, Fredericton, New Brunswick, Canada, E3B 6C2
q.k.hassan@unb.ca; cbourque@unb.ca; fmeng@unb.ca
[2] Lanzhou Regional Climate Centre, 2070 Donggang East Road, Lanzhou, 730020, Gansu, P.R. China

Abstract. This paper describes a procedure for mapping long-term average, growing season-accumulated growing degree days at an enhanced spatial resolution of 28.5 m. GDD-product enhancement is based on augmenting a previously developed 1 km resolution map of GDD described in Hassan *et al.* [*J. Applied Remote Sens.,* **1**, 013511, 12p (2007)] using data from a series of scene- and date-specific Landsat-7 ETM+ images (at 28.5 m resolution) from the 1999-2002 data collection period and a chronological series of standard MODIS 16-day composites of enhanced vegetation index (EVI; at 250 m resolution) spanning the 2003-2005 growing periods (April-October). Surface reflectances from the Landsat-7 ETM+ images are used to derive fine-scale estimates of EVI, which are then transformed into long-term averages by taking into account growing-season specific, temporal trends in the series of MODIS-EVI images. As values from the 8-day accumulated GDD and 16-day composites of EVI have been shown to be strongly correlated, a new data-fusion method based on the mean and instantaneous values of fine-grain long-term average EVI is used to augment the resolution of the initial GDD map. As a demonstration, we apply the procedure to satellite and climate station data for the Canadian Province of Nova Scotia.

Keywords: enhanced vegetation index, data fusion, growing degree days, Landsat-7 ETM+, MODIS, statistical properties

1 INTRODUCTION

Growing degree day (GDD) is an air temperature-based index commonly used in plant growth and crop production modeling [1] mainly because of temperature's role in regulating plant processes, such as evapotranspiration, photosynthesis, plant respiration, in-plant water and nutrient movement, and, ultimately, plant development, phenology, and growth. GDD can be defined here as the growing-season (April-October) accumulation of the difference between the daily mean air temperature and a constant temperature threshold, below which plant growth ceases [2].

In an earlier paper [3], we described an approach to mapping a 30-year average of growing-season accumulated GDD (1971-2000) at spatial resolutions of 250 m, mostly as a function of MODIS-based products of surface temperature (at 1 km resolution) and enhanced vegetation index (EVI) concurrent with the 2003-2005 growing periods. In spite of the regional importance of the 250 m resolution map of GDD, higher resolution maps with spatial resolutions < 30 m are in high demand for still greater understanding of land-surface processes and for ecosystem management applications at sub-hectare scales. As a result of this demand, the focus of this paper is to develop a methodology to enhance the spatial resolution of GDD mapping by fusing high resolution (28.5 m), scene- and date-specific Landsat-7 ETM+-product data with lower resolution (250 m), but more frequently acquired MODIS data.

Received 24 Jul 2007; accepted 24 Sep 2007; published 28 Sep 2007 [CCC: 19313195/2007/$25.00]

Since growing-season based estimates of 8-day accumulated GDD and 16-day composites of EVI (see Table 1, for definitions) are strongly correlated [3], an initial step in our approach is to generate EVI from Landsat-7 ETM+ surface reflectances using procedures described in Huete *et al.* [4]. Although the procedures in [4] are applied specifically to processing MODIS data in the evaluation of EVI, the same procedures have been applied to Landsat data [e.g., 4-7] due to the blue (B), red (R), near infrared (NIR) bands (in the definition of EVI) near-similar bandwidth characteristics (see Table 2).

Data fusion between Landsat-7 ETM+ and MODIS image products is not original, as recently demonstrated by [9] with the fusion of surface reflectances to predict fine-scale, daily images of surface reflectance. Our approach is different from other published data fusion approaches, as our specific objective is to fuse images representing two very different, albeit related, ecological variables, i.e., EVI and GDD. For demonstration, we apply our procedure to remote sensing and GDD data collected over the eastern Canadian Province of Nova Scotia (NS), geographically located between latitudes 43° 27' N to 46° 01' N and longitudes 59° 38' W to 66° 16' W.

2 STUDY AREA AND DATA REQUIREMENTS

Canada is divided into fifteen terrestrial ecozones, generalized land-surface categories based on similar soil formation, climate, and landuse cover types described in the National Ecological Framework for Canada [10]. The Province of NS falls in the Atlantic Maritime Ecozone of eastern Canada (Fig. 1a), and is characterized by a forest-dominated landscape.

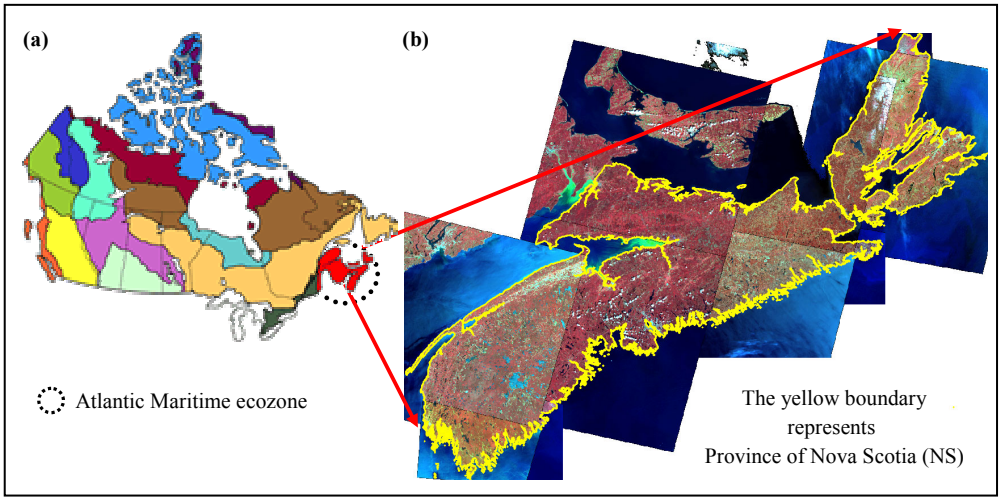

Fig. 1. Location of the Atlantic Maritime ecozone of eastern Canada (a), and a mosaic of Landsat-7 ETM+ images at 28.5 m resolution covering the Province of Nova Scotia (b).

The landscape is distinguished by its temperate evergreen-deciduous Acadian forests, where a mixture of deciduous species, such as maple (*Aceraceae* spp.), beech (*Fagus grandifolia* Ehrh.) and birch (*Betulaceae* spp.), and coniferous species, such as spruce (*Picea* spp.) and balsam fir [*Abies balsamea* (L.) Mill.] dominate. Forests occupy about 79% of the province's landbase (Natural Resources Canada; http://cfs.nrcan.gc.ca/sof/sof06/profilesNS_e.html, last visited Jun. 2007). Provincial climate is largely influenced by the region's proximity to the Bay of Fundy in the north and Atlantic Ocean to the south and east of the province. The

province experiences a cool-moist climate with an annual mean temperature and total precipitation range of 3.5-6.5°C and 900-1500 mm, respectively.

The 28.5 m resolution Landsat-7 images used in this study were acquired from the 1999-2002 data collection period from the Landsat Ecosystem Disturbance Adaptive Processing System (LEDAPS) project, i.e., http://ledaps.nascom.nasa.gov/ledaps_NorthAmerica.html, last visited June 2007. Table 1 provides a complete list and description of the data employed in the study. The 250 m resolution map of GDD developed in [3] will serve as a comparison to the spatially-enhanced map of GDD generated from this study.

Table 1. Description of the data employed in this study

Data type	Description
Landsat-7 ETM+ (surface reflectance products)	Ten scene-specific images of surface reflectance for the blue (B), red (R), and near infrared (NIR) bands covering the entire Province of NS (Fig. 1b). The path (P), row (R), and acquisition dates of the acquired scenes are as follows: **Image 01.** P6 R27 [19 Jun. 2002], **02.** P6 R28 [22 Aug. 2002], **03.** P6 R29 [22 Aug. 2002], **04.** P7 R28 [09 May 2002], **05.** P7 R29 [04 Jun. 2000], **06.** P8 R28 [13 Sep. 1999], **07.** P8 R29 [13 Sep. 1999], **08.** P8 R30 [13 Sep. 1999], **09.** P9 R29 [18 Jun. 2000], **10.** P9 R30 [18 Jul. 2000]
MODIS-based EVI products (MOD13Q1)	Thirty nine 16-day composites of EVI were acquired from NASA at 250 m resolution. The composites were derived by applying either the constrained-view angle-maximum value composite or maximum value composite algorithm (refer to [4], for detail). The 39 composites covered the 07 April-31 October, 2003 and 2005, and 06 April-30 October, 2004 April-October growing periods.
MODIS-derived product (1 km resolution map of GDD)	Derived from MODIS-based 8-day composites of surface temperature at 1 km resolution for the growing periods of 2003-2005 along with tower point-based measurements of emitted infrared radiation (refer to [3], for additional detail).
MODIS-derived product (250 m resolution map of GDD)	Derived from the 1 km resolution map of GDD. The product was generated by employing MODIS-based standard 16-day composites of EVI at 250 m resolution for the 2003-2005 period and 30-year mean point-calculations of GDD (for the 1971-2000 period) for 101 climate stations [3].

3 METHODOLOGY

Figue 2 shows a schematic diagram for generating a 30-year average map of GDD at 28.5 m resolution from an initial GDD map at 1 km resolution [3]. The procedure is divided into three main components, namely *(i)* computing EVI from Landsat-7 ETM+ surface reflectances of the B, R, and NIR bands, and transforming day-specific Landsat-7 ETM+-derived EVI values to long-term averages using MODIS-derived values for the 2003-2005 period (addressed in Section 3.1, below), *(ii)* fusing long-term average EVI values with the 1 km resolution map of GDD, and *(iii)* generating a GDD map at enhanced resolution for the current normal period (1971-2000).

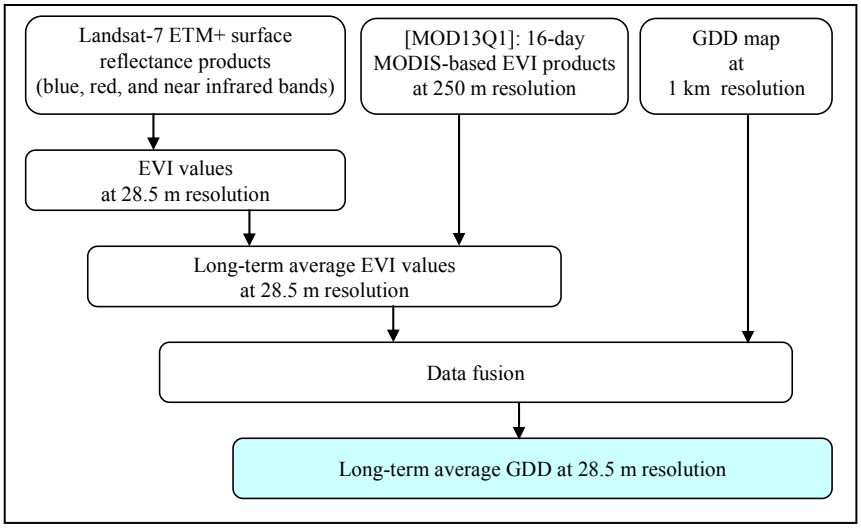

Fig. 2. Procedural diagram for generating a long-term map of GDD at 28.5 m resolution for the 1971-2000 current normal period.

3.1 Long-term average EVI from Landsat-7 ETM+ data

Since Landsat-7 ETM+ surface reflectances were already corrected for atmospheric distortions [8], we proceeded by determining EVI values for each Landsat-7 ETM+ scene with

$$EVI = 2.5\frac{\rho_{NIR} - \rho_R}{\rho_{NIR} + 6\ x\ \rho_R - 7.5\ x\ \rho_B + 1}\ , \qquad (1)$$

(after [4]), where ρ is the atmospherically-corrected surface reflectance for B, R, and NIR bands, respectively. The application of Eq. (1) for computing EVI using Landsat-7 ETM+ images would be considered reasonable, as surface reflectances measured with the Landsat-7 ETM+ and MODIS sensors were generally comparable [8]; only showing minor differences, despite some variation in sensor bandwidths (Table 2).

Table 2. Landsat-7 ETM+ and MODIS sensor bandwidths for B, R, and NIR bands.

Band	**Landsat-7 ETM+** (μm)	**MODIS** (μm)
B	0.450-0.520	0.459-0.479
R	0.630-0.690	0.620-0.670
NIR	0.780-0.900	0.841-0.876

To calculate long-term average EVI at 28.5 m resolution, we used the following steps,

(i) Using MODIS-based EVI products, we computed pixel-level averages of growing-season EVI for the 2003-2005 growing periods at 250 m resolution. Following that we computed a single EVI value (i.e., $\overline{EVI}_{MODIS}$) by spatially averaging growing-season pixel EVI averages;

(ii) We then calculated Landsat-7 ETM+ scene-specific spatial averages of EVI (one for each scene); and

(iii) For each Landsat-7 ETM+ image, pixel-level averages of EVI were obtained using

$$EVI_{Long-term}(i) = EVI_{ETM}(i) - \left(\overline{EVI}_{ETM}(i) - \overline{EVI}_{MODIS} \right), \quad (2)$$

where i is the scene number (1-10), $EVI_{Long-term}$ the long-term average EVI at 28.5 m resolution (expected outcome), EVI_{ETM} instantaneous values of EVI for individual pixels based on Landsat-7 ETM+ image data, and $\overline{EVI}_{ETM}$ the average Landsat-7 ETM+ scene-specific EVI values. $\overline{EVI}_{MODIS}$ in Eq. (2) represents a regional value of EVI for the 2003-2005 growing periods [Step (i), above].

As the estimated EVI values derived from MODIS and Landsat-7 ETM+ data have near-similar magnitude [4], we can apply the difference between the average EVI values in Eq. (2) (i.e, $\overline{EVI}_{ETM}$ and $\overline{EVI}_{MODIS}$) as a correction to the Landsat-7 ETM+ -based instantaneous values of EVI to yield long-term mean values of EVI at 28.5 m resolution.

3.2 Data fusion

In order to enhance the spatial resolution of the GDD map, we developed a new data fusion technique. This consisted of generating an artificial image plane (AI) which took into account the statistical properties of Landsat-7 ETM+-based $EVI_{Long-term}$ within a 3 cell × 3 cell moving window, i.e.,

$$AI = \frac{EVI_{ins}}{EVI_{mean}}, \quad (3)$$

where EVI_{ins} is the instantaneous value of EVI and EVI_{mean} is the mean of $EVI_{Long-term}$ within the moving window. In theory, AI is an index that describes the relation of an instantaneous value of EVI to the mean value of EVI of surrounding pixels, and functions as a weight in the calculation of GDD at 28.5 m resolution, i.e.,

$$GDD_{28.5\ m} = AI \times GDD_{1\ km}, \quad (4)$$

where $GDD_{1\ km}$ represents the initial GDD map derived from MODIS-surface temperature data at 1 km resolution [3].

3.3 Long-term average GDD at 28.5 m resolution for the current normal period

The GDD map produced using Eq. (4) was modified by setting a lower and upper limit to the GDD values generated. GDD values ≤ 800 were set to 800 as these values were typically observed over water and along the coastal border of the province. Values ≥ 2500 were set to 2500 as these values were mostly associated with urbanized centres with restricted plant cover and elevated surface heating. These limits were justified given the focus was to study temperature and GDD patterns over vegetated surfaces. As in [3], we applied a constant correction of -511 to the three-year GDD map (2003-2005) to generate a final, GDD map at 28.5 m resolution for the 1971-2000 normal period. This constant offset was determined by

comparing GDD values estimated from 101 Environment Canada climate stations for the current normal period to GDD point-estimates estimated from 2003-2005 MODIS data.

4 RESULTS AND DISCUSSION

Figure 3 shows the interannual variation of regionally-averaged EVI values (at 250 m resolution) determined from MODIS data. Strong seasonal influences were borne out when the data was fitted with a quadratic function, producing r^2-values ≥ 86%.

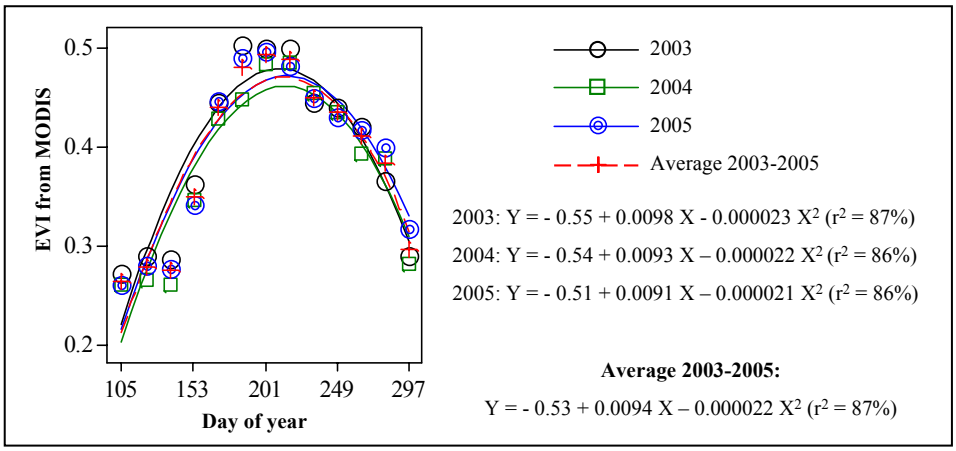

Fig. 3. Interannual variation of regionally-averaged MODIS-based EVI values for the 2003-2005 period.

Figure 4 shows a sample calculation using our data fusion approach on 2003-2005 computations. A 997.5 m × 997.5 m pixel-calculation of GDD at 28.5 m resolution provided a mean GDD value of 1872 compared with 1881 from the original MODIS-based calculations at 1 km resolution ([3]; Fig. 4a). This difference was most likely due to the greater detail (and therefore variability) expressed in the 28.5 m resolution data with compare to the 1 km resolution data.

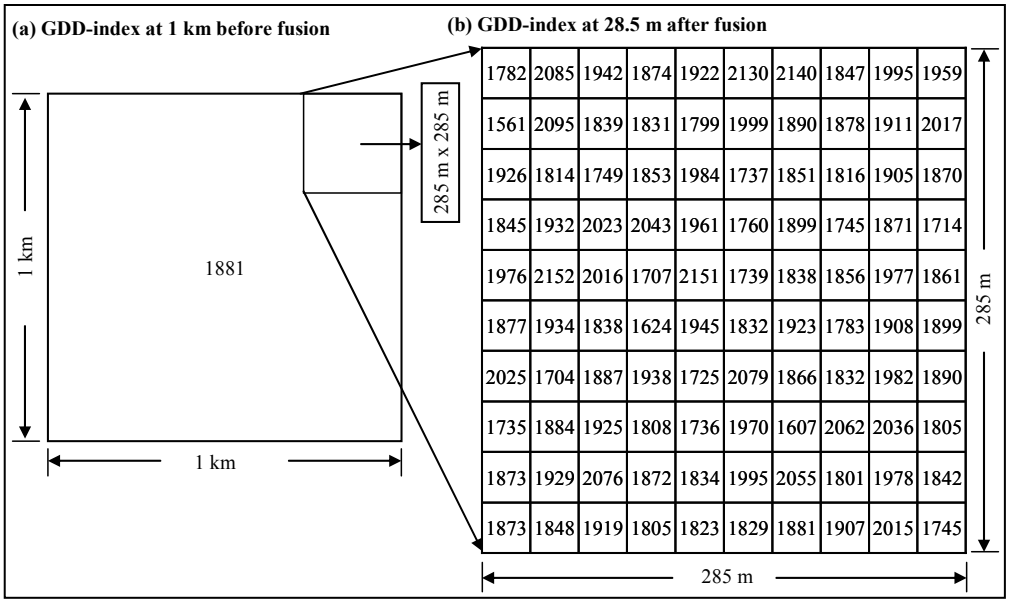

Fig. 4. Comparison of GDD values obtained without and with data fusion applied.
Mean GDD value at 1 km resolution is 1881 and at 28.5 m, 1872.

Figure 5 shows the spatially enhanced long-term average GDD map for the current normal period (Fig. 5a) and associated GDD frequency distribution (Fig. 5b) at 28.5 m for the province of NS. For validation purposes, we opted to use our previously generated MODIS-based GDD map at 250 m resolution [3], as it was calibrated and validated using two independent datasets, namely, GDD values from Environment Canada climate stations and a GDD map for the 1951-1980 normal period (Ref. 11-12). Fig. 5c provides a comparison of GDD pixel values for the 250 m resolution map with the mean values obtained by averaging the pixel values of the current map (at 28.5 m resolution) coinciding with individual 250 m × 250 m pixels. Despite slight variations between pixel values at 1 km resolution (Fig. 4), mean values and spatial distribution for the two maps were nearly identical. This was borne out by the alignment of comparison data pairs specified at 250 m resolution along the 1:1 correspondence line and linear regression statistics of the line fitted to the data (i.e., slope of 0.90, y-intercept of 143.93, and an r^2-value of 99.6%; Fig. 5c). Greatest systematic deviation from the 1:1 correspondence line occurred for values in the 800-1000 and 1700+ ranges. The 800-1000 range corresponded to observations made over discontinuous wetland, riparian forests, and low-lying wet zones, while values > 1700 coincided with agricultural zones and sparse vegetation areas. This deviation was most likely related to the reduction in variation (and detail) associated with the lower resolution MODIS-based GDD map.

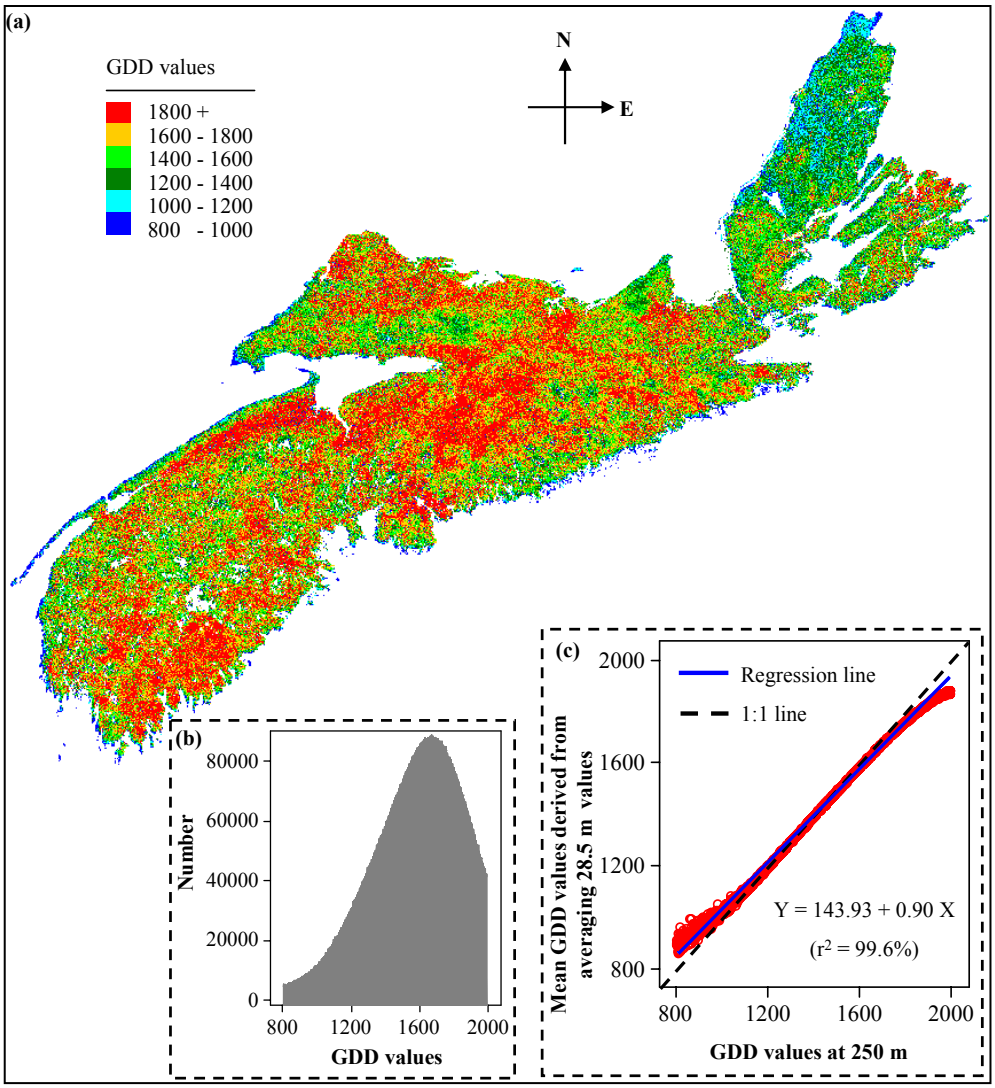

Fig. 5. (a) Spatial and (b) frequency distribution of long-term average GDD at 28.5 m resolution for the current normal period (1971-2000); and (c) comparison of GDD values obtained by averaging values at 28.5 m coincident with individual 250 m × 250 m pixels (y-axis) and values originally derived at 250 m resolution (x-axis, based on work described in [3]).

5 CONCLUDING REMARKS

In this paper, we demonstrated an approach for generating a long-term average GDD map at an enhanced resolution of 28.5 m for the current normal period using Landsat-7 ETM+ surface reflectance products at 28.5 m resolution, MODIS-based EVI products at 250 m resolution, and a previously-derived GDD map generated primarily from MODIS-based surface temperature products at 1 km resolution. The core of the methodology is based on a new statistical data fusion approach by exploiting the underlying relationship between EVI and GDD. Although there were pixel-level variations in calculated GDD, spatial patterns at

regional scales remained mostly unaffected. This data fusion approach has potential to be used in fusing ecological data collected, or processed from data collected, from different remote sensing platforms with bands of near-similar characteristics.

Acknowledgments

This study was partially funded by the Fluxnet-Canada Research Network (FCRN) project, Department of Natural Resources of the Province of Nova Scotia, Canada and funds from a Discovery Grant awarded to CPAB from the Natural Science and Engineering Council of Canada (NSERC). We would like to acknowledge NASA and the LEDAPS project for providing MODIS and Landsat-7 ETM+ surface reflectance data free of charge.

References

[1] C. P. -A. Bourque, F. -R. Meng, J. J. Gullison, and J. Bridgland, "Biophysical and potential vegetation growth surfaces for a small watershed in northern Cape Breton Island, Nova Scotia, Canada," *Can. J. For. Res.* **30**, 1179–1195 (2000) [doi:10.1139/cjfr-30-8-1179].

[2] B. Li, S. Tao, R. W. Dawson, "Relations between AVHRR NDVI and ecoclimatic parameters in China," *Int. J. Remote Sens.* **23**, 989–999 (2002) [doi:10.1080/014311602753474192].

[3] Q. K. Hassan, C. P.-A. Bourque, F.-R. Meng, and W. Richards, "Spatial mapping of growing degree days: an application of MODIS-based surface temperatures and enhanced vegetation index," *J. Appl. Remote Sens.*, **1**, 013511, 12p (2007) [doi:10.1117/1.2740040].

[4] A. Huete, K. Didan, T. Miura, E. P. Rodriguez, X. Gao, L. G. Ferreira, "Overview of the radiometric and biophysical performance of the MODIS vegetation indices," *Remote Sens. Environ*. **83**, 195–213(2002) [doi:10.1016/S0034-4257(02)00096-2].

[5] Y. Ogud, Y. Sugal, S. Takeuchi, K. Ogawa, and K.Tsuchiya, "Monitoring of a rice field using Landsat-5 TM and Landsat-7 ETM+ data," *Adv. Space Res.* **32**, 2223-2228 (2003).

[6] X. Chen, L. Vierling, E. Rowell, and T. DeFelice, "Using lidar and effective LAI data to evaluate IKONOS and Landsat 7 ETM+ vegetation cover estimates in a ponderosa pine forest," *Remote Sens. Environ.* **91**, 14–26 (2004).

[7] W. M. Baugh, and D. P. Groeneveld, "Broadband vegetation index performance evaluated for a low-cover environment," *Int. J. Remote Sens.* **27**, 4715 – 4730 (2006).

[8] J. G. Masek, E. F. Vermote, N. E. Saleous, R. Wolfe, F. G. Hall, F. Huemmrich, F. Gao, J. Kutler, and T.-K. Lim, "A Landsat surface reflectance data set for North America, 1990–2000," *IEEE Geosci. Remote Sens. Lett.*, **3**, 69–72 (2006) [doi:10.1109/LGRS.2005.857030].

[9] F. Gao, J. Masek, M. Schwaller, and F. Hall, "On the Blending of the Landsat and MODIS Surface Reflectance: Predicting Daily Landsat Surface Reflectance," *IEEE Trans Geosci. Remote Sens.*, **44**, 2207-2218 (2006) [doi:10.1109/TGRS.2006.872081].

[10] Ecological Stratification Working Group. *A National Ecological Framework for Canada*. Agriculture and Agri-Food Canada, Research Branch, Centre for Land and Biological Resources Research and Environment Canada, State of Environment Directorate, Ottawa/Hull, (1996).

[11] P. A. Dzikowski, G. Kirby, G. Read, and W. G. Richards, *The climate for agriculture in Atlantic Canada*, For the Atlantic Advisory Committee on Agrometeorology, Publication No. ACA 84-2-500, Agdex No. 070 (1984).

[12] The Ecosystem Classification Working Group. *Our landscape heritage: the story of ecological land classification in New Brunswick.* Department of Natural Resources and Energy, New Brunswick, Canada (2003).

Quazi K. Hassan is currently a PhD candidate and research assistant at the University of New Brunswick. He received a BSc in electrical and electronic engineering from Bangladesh Institute of Technology (BIT), Khulna, Bangladesh (presently known as Khulna University of Engineering and Technology, Bangladesh), and an MSc in remote sensing and GIS from University Putra Malaysia. His research interests include the use of remote sensing data in the fields of forestry and other natural resources, flood mapping and monitoring, land use mapping, river morphology, and coastal area mapping, among others.

Charles P.-A. Bourque is Professor of forest hydrometeorology at the University of New Brunswick. Dr. Bourque received his BSc (Hons) from Dalhousie University, Canada, in mathematics and theoretical ecology. He also received a second BSc in Dynamic Meteorology from the University of Alberta, Canada, an MSc and a PhD from the University of New Brunswick, Canada in forest meteorology and environmental sciences. Dr Bourque's research interests include systems modelling, eddy covariance measurement of biospheric fluxes, and landscape process modelling.

Fan-Rui Meng is a Professor of forest watershed management at the University of New Brunswick. Dr. Meng received a BSc in forest engineering and an MSc in forest planning from Northeast Forestry University, China, and a PhD in forest ecology from the University of New Brunswick, Canada. Dr. Meng's research interests include ecological modelling, forest watershed management, and forest hydrology.